

Temporal variability of the anthropogenic CO₂ storage in the Irminger Sea

F. F. Pérez¹, M. Vázquez-Rodríguez¹, E. Louarn^{2,3}, X. A. Padín¹, H. Mercier⁴, and A. F. Ríos¹

¹Instituto de Investigaciones Marinas, CSIC, Eduardo Cabello 6, 36208 Vigo, Spain

²Laboratoire de Chimie Marine, Institut Universitaire Européen de la Mer, Plouzané, France

³Station Biologique de Roscoff, CNRS UPMC, B.P. 74, 29682 Roscoff, France

⁴Laboratoire de Physique des Océans, CNRS Ifremer IRD UBO, IFREMER Centre de Brest, B.P. 70, 29280 Plouzané, France

Received: 29 February 2008 – Published in Biogeosciences Discuss.: 11 April 2008

Revised: 14 November 2008 – Accepted: 14 November 2008 – Published: 11 December 2008

Abstract. The anthropogenic CO₂ (C_{ant}) estimates from cruises spanning more than two decades (1981–2006) in the Irminger Sea area of the North Atlantic Subpolar Gyre reveal a large variability in the C_{ant} storage rates. During the early 1990's, the C_{ant} storage rates ($2.3 \pm 0.6 \text{ mol C m}^{-2} \text{ yr}^{-1}$) doubled the average rate for 1981–2006 ($1.1 \pm 0.1 \text{ mol C m}^{-2} \text{ yr}^{-1}$), whilst a remarkable drop to almost half that average followed from 1997 onwards. The C_{ant} storage evolution runs parallel to chlorofluorocarbon-12 inventories and is in good agreement with C_{ant} uptake rates of increase calculated from sea surface pCO₂ measurements. The contribution of the Labrador Seawater to the total inventory of C_{ant} in the Irminger basin dropped from 66% in the early 1990s to 49% in the early 2000s. The North Atlantic Oscillation shift from a positive to a negative phase in 1996 led to a reduction of air-sea heat loss in the Labrador Sea. The consequent convection weakening accompanied by an increase in stratification has lowered the efficiency of the northern North Atlantic CO₂ sink.

on average) of all oceans, holding 38% of the oceanic C_{ant} inventory (Sabine et al., 2004). The key mechanism responsible for this large CO₂ uptake is the Meridional Overturning Circulation (MOC). The MOC transports warm surface waters with high C_{ant} loads from low latitudes to the northern North Atlantic (Watson et al., 1995; Wallace et al., 2001), where the deep convection and entrainment by the overflows contribute to store this C_{ant}-laden water at depth. Eventually, these waters will return south in the lower limb of the MOC. Recent studies on the variability of the MOC point towards a possible decrease in its intensity during the second half of the twentieth century (Bryden et al., 2005). The causes for it are mainly attributed to the greenhouse-enhanced temperature rise and freshwater flux in high latitudes, where water mass formation processes abound. Based on multi-model simulations, an average MOC reduction of 25% (0–50%) by year 2100 under a SRES emission scenario A1B is very likely to occur (IPCC, 2007). The slowdown of MOC would bring forth profound consequences for global climate due to the associated decrease in heat transport (Drijfhout et al., 2006) and oceanic C_{ant} uptake (Sarmiento and Le Quéré, 1996). However, regarding the oceanic sequestration of C_{ant} it must be noted that the possibility of the MOC shutting down and its consequences are not free of ambiguity. Joos et al. (1999) have reported that the projected changes of the marine biological cycle compensate the reduction in downward mixing of C_{ant}, except when the North Atlantic thermohaline circulation collapses. Moreover, Duce et al. (2008) have argued that the predicted enhanced downward organic carbon fluxes in MOC shutdown scenarios, driven by anthropogenic nitrogen, could actually compensate for and even increase the oceanic uptake of C_{ant}. Several Ocean General Circulation Models (OGCMs) have suggested that the decadal variability of the

1 Introduction

The ocean is a CO₂ sink that during the 1990s has removed $2.2 \pm 0.4 \text{ Pg C yr}^{-1}$ from the atmosphere out of the total $8.0 \pm 0.5 \text{ Pg C yr}^{-1}$ of anthropogenic carbon (C_{ant}) emitted to the atmosphere directly from human activities (Canadell et al., 2007). The North Atlantic Subpolar Gyre (NASPG) has the largest C_{ant} inventory per unit area ($\sim 80 \text{ mol C m}^{-2}$



Correspondence to: F. F. Pérez
(fiz.perez@iim.csic.es)

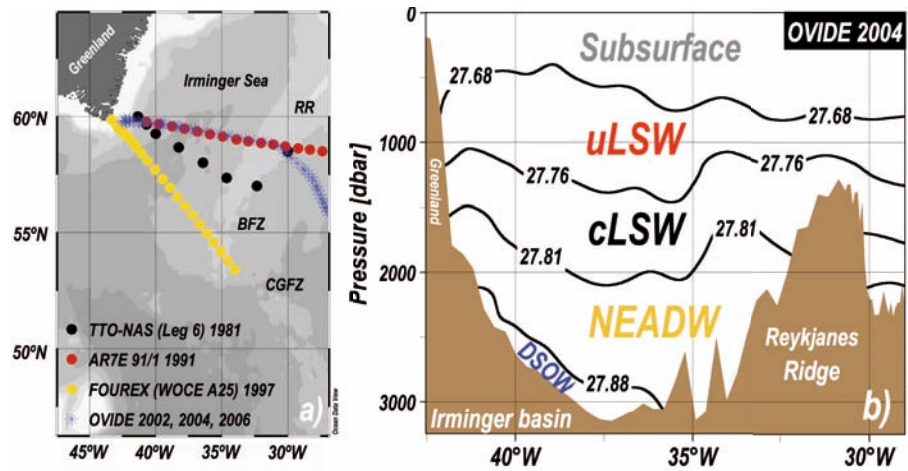


Fig. 1. (a) Map showing the Irminger Sea ends of the North Atlantic cruises used to assess the temporal evolution of the Cant storage. The acronyms stand for: R = Reykjanes Ridge, BFZ = Bight Fracture Zone and CGFZ = Charlie Gibbs Fracture Zone. (b) Main water masses (cLSW = classical Labrador Seawater; uLSW = upper Labrador Seawater; NEADW = North East Atlantic Deep Water; DSOW = Denmark Strait Overflow Water) present in the Irminger basin and analysed in terms of C_{ant} inventory distributions over time. The density (σ_{θ} , in kg m^{-3}) boundaries were established following Kieke et al. (2007) and Yashayaev et al. (2008).

MOC is closely related with the variability of Labrador Seawater (LSW) formation rates (Hátún et al., 2005; Latif et al., 2006; Böning et al., 2006). On the other hand, the long-term evolution of the MOC such as the possible weakening during the 21st century might be related to a decrease in the density of the Denmark Strait Overflow Water (DSOW) and the Iceland-Scotland Overflow Water (ISOW) (Cubasch et al., 2001; IPCC, 2007; Böning et al., 2006). These water masses meet in the Irminger Sea, where the Deep Western Boundary Current originates (Yashayaev et al., 2008, hereinafter Y'08).

The Irminger basin has been proposed as a LSW formation region (Pickart et al., 2003; Falina et al., 2008), in addition to the Labrador Sea. Independently of the formation region, two modes of LSW are typically defined: the classical LSW (cLSW, sometimes referred to as deep LSW) and the less dense upper LSW (uLSW) (Pickart et al., 1997). The LSW is formed in winter, when deep convection caused by intense air-sea heat loss results in the formation of homogeneous layers that can exceptionally reach depths of up to 2000 m (Kieke et al., 2006, hereinafter K'06). The ambient stratification and wind forcing intensity are determinant factors in this convective process (Dickson et al., 1996; Curry et al., 1998; Lazier et al., 2002). The convection activity in the Labrador Sea is related to the persistence and phase of the North Atlantic Oscillation (NAO) index. A positive NAO phase causes the intensification of winds and heat loss (surface cooling) in the Labrador Sea, fostering convection processes. During the early 1990's, the strongly positive NAO index forced an impressive and exceptional convection activity down to more than 2000 m (Dickson et al., 1996; Lazier et al., 2002; Häkkinen et al., 2004; Y'08). This resulted in the formation of the thickest layer of cLSW observed in

the past 60 years (Curry et al., 1998). This energetic convection period abruptly ended in 1996 with the shift of the NAO index to a negative phase. Nonetheless, weaker convection events (to less than 1000 m depth on average) continued to take place in the central Labrador Sea and formed the less dense uLSW. This water mass was first detected and described by Pickart et al. (1997) in the western Labrador Sea. Alternatively, the uLSW was spotted successively during the second half of the 1990's (Azetsu-Scott et al., 2003, hereinafter AS'03; Stramma et al., 2004). Decadal time series of layer thicknesses of both LSW types corroborate that, far from exceptional, uLSW is an important product of the convection activity in the Labrador Sea (K'06). These time series show that the strong formation processes of cLSW in the early 1990's are actually the exceptional events. The observations point to a slight chlorofluorocarbon-12 (CFC12) concentration decline (within the analytical uncertainty range, though) towards the end of the decade in the cLSW body (AS'03), following a strong CFC12 concentration increase that occurred in the early 1990s. This CFC12 decrease was also observed during the early 2000's in the Labrador and Irminger Seas (Kieke et al., 2007, hereinafter K'07). The fluctuations of convection in the NASPG can modify the expected oceanic C_{ant} uptake rates in a likewise and parallel manner to CFCs.

In this study we have gathered hydrographical measurements and results from six cruises conducted in the Irminger Sea. The aim is twofold: a) study the evolution of C_{ant} concentrations in sub-surface waters, LSW, North East Atlantic Deep Water (NEADW) and DSOW in order to b) evaluate the variability of the oceanic storage rates of C_{ant} linked to the fluctuations of the convective processes in the NASPG, and the reduction of the formation of cLSW.

Table 1. Summary of cruises showing the analytical precision of the measurements for the main variables used in C_{ant} estimation. N stands for the number of NM means “Not Measured” and NA stands for “No Adjustment made”. In any case, units for C_T , A_T and oxygen (O) are in $\mu\text{mol kg}^{-1}$.

Cruise	Date	P.I.	No. of Stations	No. of Samples	Analytical Precision				Adjustment	
					C_T	A_T	pH	O	C_T	A_T
TTO-NAS	23/07–14/08/1981	T. Takahashi	7	140	± 3.5	± 3.7	NM	± 1.0	–3.0	–3.6
AR7E 91/1	08/04–02/05/1991	H. M. van Aken	10	216	± 2.0	NM	NM	± 0.5	NA	NA
FOUREX	07/08–17/09/1997	S. Bacon	17	327	± 3.0	± 2.0	± 0.002	± 1.0	NA	NA
OVIDE 02	11/06–11/07/2002	H. Mercier	17	356	± 3.0	± 2.0	± 0.002	± 0.5	NA	NA
OVIDE 04	05/06–06/07/2004	T. Huck	17	395	± 3.0	± 2.0	± 0.002	± 0.5	NA	NA
OVIDE 06	24/05–26/06/2006	P. Lherminier	21	444	± 3.0	± 2.0	± 0.002	± 0.5	NA	NA

2 Dataset and method

Six cruises spanning through 25 years (1981–2006) of high-quality carbon measurements in the Irminger Sea area have been selected for this study. These are the TTO-NAS leg 4¹, AR7E 91/1², FOUREX/WOCE A25³ and the OVIDE 2002, 2004 and 2006 cruises (Fig. 1a, Table 1). The bottle and CTD data yielded very similar property profiles. Since bottle data includes all carbon-related analysis, only bottle data was used in this study. Unlike in the most recent cruises of FOUREX or throughout the OVIDE project, the TTO-NAS and AR7E 91/1 analytics did not include certified reference materials for their total inorganic carbon (C_T) measurements. For the TTO-NAS, Tanhua et al. (2005) performed a cross-over analysis with an overlapping more recent cruise. Based on a comparison with modern Certified Reference Material-referenced data, they suggest a correction for TTO-NAS C_T measurements of $-3.0 \mu\text{mol kg}^{-1}$, which has been applied to our dataset. In order to evaluate and interpret the variations of C_{ant} rates of storage we have focused on six water masses delimited by the density (σ_θ) intervals established following K’07 and Y’08, namely: from the upper 100 m to $\sigma_\theta=27.68 \text{ kg m}^{-3}$ we find the sub-surface layer; The uLSW is found between $27.68 < \sigma_\theta < 27.76 \text{ kg m}^{-3}$; cLSW between $27.76 < \sigma_\theta < 27.81 \text{ kg m}^{-3}$; North East Atlantic Deep Water (NEADW, which includes the ISOW contributions) is delimited by $27.81 < \sigma_\theta < 27.88 \text{ kg m}^{-3}$, and DSOW by $\sigma_\theta > 27.88 \text{ kg m}^{-3}$ (Fig. 1b).

To estimate the anthropogenic CO₂ the φC_T° method from Vázquez-Rodríguez et al. (2008a) is applied (refer to Appendix A for details). It is a data-based, back-calculation method that constitutes an alternative version of the classical ΔC^* approach (Gruber et al., 1996). The φC_T° method is not CFC-reliant and uses sub-surface layer (100–200 m)

¹<http://cdiac3.ornl.gov/waves/>

²http://whpo.ucsd.edu/data/repeat/atlantic/ar07e/ar07ea/ar07e_a_hy1.csv

³<http://whpo.ucsd.edu/data/onetime/atlantic/a25/index.htm>

data from the whole Atlantic as the only reference to build the parameterizations needed. This sub-surface layer avoids the seasonal variability of surface properties, thus making the derived parameterizations more representative of water mass formation conditions. The method also takes into account the temporal variation of the CO₂ air-sea disequilibrium (ΔC_{dis}). The overall uncertainty of the method has been estimated in $5.2 \mu\text{mol kg}^{-1}$ by means of random error propagation over the precision limits of the parameters involved in the calculation of C_{ant} (refer to Appendix A). Regarding the specific inventory estimates, errors were estimated using a perturbation procedure for each layer and the total water column. They were calculated by means of random propagation with depth of a $5.2 \mu\text{mol kg}^{-1}$ standard error of the C_{ant} estimate over 100 perturbation iterations, and are given in Table 2. Assuming that the uncertainties attached to the C_{ant} estimation method are purely random and do not introduce biases, the final error included in Fig. 4 is calculated by propagating the individual errors associated to the samples. They reflect both measurement and parameterization errors.

3 Results

The fields of potential temperature (θ), salinity (S), apparent oxygen utilisation (AOU, the difference between the saturated and measured concentrations of oxygen) and C_{ant} in the Irminger Basin from 1981 to 2006 are shown in Fig. 2. The TTO-NAS section shows a strong vertical stratification at the LSW level between the first 1000 m and the relative salinity maximum of the NEADW (> 34.95), related to the low convection activity in the Labrador Sea in the late 1970’s (K’06). This can derive from the fact that it takes two years for the LSW to spread into the Irminger Sea (Y’08). The temperature minimum ($\theta < 1.5^\circ\text{C}$) in the DSOW is also remarkable within the considered time-span. Compared to TTO-NAS, the AR7E (1991) cruise shows cooler LSW. The strong vertical homogenisation down to 1800 m in 1991 suggests local

Table 2. Temporal evolution (1981–2006) of the average values of thickness (\pm STD), salinity, potential temperature, AOU, C_{ant}, percentage of C_{ant}^{sat} and percentage contribution to the specific inventory of C_{ant} in the five considered water masses. The averages come from bottle data and the uncertainties stand for the error of the mean. Total specific inventories are given by the red line in Fig. 4.

Year	Thickness (m)	Salinity	θ (°C)	AOU ($\mu\text{mol kg}^{-1}$)	C _{ant} ($\mu\text{mol kg}^{-1}$)	%C _{ant} ^{sat}	%Inventory
Sub-surface layer							
1981	419 \pm 410	34.902 \pm 0.001	5.118 \pm 0.005	20.4 \pm 0.3	29.3 \pm 1.5	95 \pm 5	22.6 \pm 1.1
1991	144 \pm 141	34.981 \pm 0.002	5.229 \pm 0.007	19.0 \pm 0.4	34.6 \pm 1.8	92 \pm 5	8.0 \pm 0.4
1997	414 \pm 406	34.893 \pm 0.001	5.134 \pm 0.003	21.0 \pm 0.1	38.8 \pm 0.8	92 \pm 2	20.7 \pm 0.4
2002	405 \pm 397	34.949 \pm 0.001	5.362 \pm 0.003	24.6 \pm 0.2	42.1 \pm 0.8	90 \pm 2	22.3 \pm 0.4
2004	556 \pm 544	34.967 \pm 0.001	5.611 \pm 0.002	23.8 \pm 0.1	43.5 \pm 0.6	89 \pm 1	30.3 \pm 0.4
2006	552 \pm 540	34.973 \pm 0.001	5.587 \pm 0.002	23.7 \pm 0.1	43.4 \pm 0.6	86 \pm 1	29.6 \pm 0.4
uLSW							
1981	829 \pm 811	34.865 \pm 0.001	3.539 \pm 0.004	28.1 \pm 0.2	25.2 \pm 1.2	84 \pm 5	38.4 \pm 1.8
1991	713 \pm 698	34.889 \pm 0.001	3.577 \pm 0.004	24.2 \pm 0.2	31.3 \pm 0.9	86 \pm 3	35.8 \pm 1.0
1997	506 \pm 496	34.869 \pm 0.001	3.520 \pm 0.003	35.9 \pm 0.1	32.1 \pm 0.7	79 \pm 2	21.0 \pm 0.4
2002	686 \pm 671	34.896 \pm 0.001	3.803 \pm 0.003	35.0 \pm 0.1	33.7 \pm 0.6	75 \pm 2	30.2 \pm 0.5
2004	673 \pm 659	34.888 \pm 0.001	3.710 \pm 0.003	37.2 \pm 0.1	33.2 \pm 0.7	71 \pm 2	27.9 \pm 0.6
2006	646 \pm 633	34.901 \pm 0.001	3.822 \pm 0.002	34.1 \pm 0.1	34.4 \pm 0.6	70 \pm 2	27.5 \pm 0.4
cLSW							
1981	557 \pm 546	34.918 \pm 0.002	3.375 \pm 0.006	39.2 \pm 0.4	18.6 \pm 1.7	62 \pm 9	19.1 \pm 1.8
1991	970 \pm 948	34.878 \pm 0.001	3.137 \pm 0.004	32.5 \pm 0.2	24.6 \pm 0.9	68 \pm 3	38.1 \pm 1.3
1997	983 \pm 960	34.868 \pm 0.001	2.989 \pm 0.003	30.8 \pm 0.1	29.9 \pm 0.7	74 \pm 2	37.8 \pm 0.9
2002	678 \pm 663	34.897 \pm 0.001	3.185 \pm 0.003	38.8 \pm 0.2	27.2 \pm 0.7	61 \pm 3	24.1 \pm 0.6
2004	546 \pm 534	34.902 \pm 0.001	3.232 \pm 0.004	40.5 \pm 0.2	26.8 \pm 0.9	58 \pm 3	18.3 \pm 0.6
2006	529 \pm 518	34.920 \pm 0.001	3.355 \pm 0.003	40.6 \pm 0.2	27.1 \pm 0.8	56 \pm 3	17.8 \pm 0.5
NEADW							
1981	686 \pm 672	34.948 \pm 0.001	2.980 \pm 0.004	44.3 \pm 0.3	14.1 \pm 1.2	47 \pm 9	17.7 \pm 1.6
1991	746 \pm 730	34.940 \pm 0.001	2.925 \pm 0.003	48.4 \pm 0.1	12.9 \pm 0.8	36 \pm 6	15.4 \pm 0.9
1997	754 \pm 738	34.924 \pm 0.001	2.813 \pm 0.004	44.2 \pm 0.2	18.5 \pm 1.0	46 \pm 5	18.0 \pm 0.9
2002	762 \pm 745	34.917 \pm 0.001	2.759 \pm 0.002	43.7 \pm 0.1	20.7 \pm 0.7	47 \pm 3	20.6 \pm 0.7
2004	755 \pm 739	34.916 \pm 0.001	2.753 \pm 0.003	44.4 \pm 0.2	21.7 \pm 0.8	47 \pm 4	20.5 \pm 0.8
2006	787 \pm 770	34.929 \pm 0.001	2.850 \pm 0.003	43.2 \pm 0.1	22.1 \pm 0.8	46 \pm 3	21.5 \pm 0.7
DSOW							
1981	98 \pm 96	34.892 \pm 0.002	1.680 \pm 0.010	36.6 \pm 0.4	12.7 \pm 2.5	43 \pm 20	2.3 \pm 0.4
1991	134 \pm 131	34.897 \pm 0.001	1.778 \pm 0.005	41.6 \pm 0.2	12.7 \pm 1.2	36 \pm 9	2.7 \pm 0.3
1997	94 \pm 93	34.894 \pm 0.002	1.720 \pm 0.008	38.8 \pm 0.4	19.8 \pm 2.2	50 \pm 11	2.4 \pm 0.3
2002	110 \pm 108	34.887 \pm 0.001	1.721 \pm 0.004	39.4 \pm 0.2	18.7 \pm 1.3	43 \pm 7	2.7 \pm 0.2
2004	112 \pm 110	34.869 \pm 0.001	1.534 \pm 0.004	36.3 \pm 0.2	21.1 \pm 1.1	47 \pm 5	3.0 \pm 0.2
2006	132 \pm 129	34.906 \pm 0.001	1.866 \pm 0.005	37.6 \pm 0.2	21.6 \pm 1.0	46 \pm 4	3.5 \pm 0.2

LSW formation at the Irminger Sea (Pickart et al., 2003), which caused the saltier NEADW signal to shrivel. The same year, the LSW layer also thickened substantially in the Labrador Sea (Fig. 12 in K'06). Since the AR7E cruise was carried out shortly after the winter season, the sub-surface layer thickness is seen to decrease substantially (Table 2). In 1997, the low salinity LSW invaded lower layers, beyond the 2000 m depth, while surface stratification slightly increased. The temperature of the cLSW reaches its minimum values for the period of observation, in agreement with Y'08, who observed that this minimum had been developing since at least

one year earlier. The DSOW temperature signature ($\theta < 2^\circ\text{C}$) thinned considerably during the FOUREX cruise (1997), but recovered during the OVIDE cruises history, most importantly in 2004. It is likely that this variability is linked to that of the entrainment downhill of the sills. Alternatively, it must be noted that the FOUREX cruise intersects the DWBC to the south of the OVIDE line, and this may partially account for this difference. During this period of biennial sampling (2002, 2004 and 2006) an increase in salinity (especially at the LSW and NEADW layers) and stratification is observed, coinciding with a period of weak winter convection (K'06;

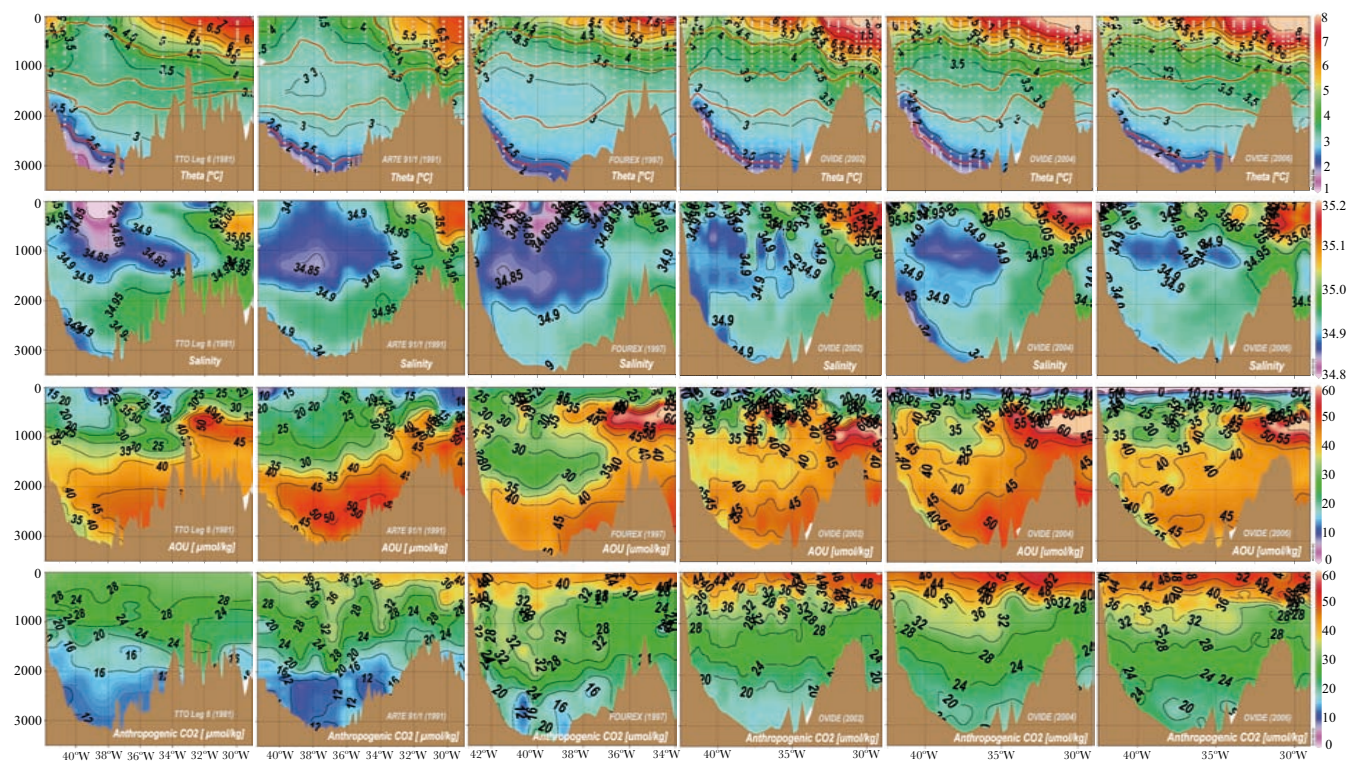


Fig. 2. Vertical profiles from bottle data of, potential temperature (Theta θ , in $^{\circ}\text{C}$), Salinity, AOU ($\mu\text{mol kg}^{-1}$) and C_{ant} ($\mu\text{mol kg}^{-1}$) for the six cruises shown in Fig. 1a. Depth is indicated in the left-hand axis in dbar. The colour scale in each of the variables is the same for all years to facilitate comparison. It must be noticed that the eastern and western ends of the different sections are not necessarily identical. The red lines in the θ plots represent the same isopycnals shown in Fig. 1b, separating the main water masses in the Irminger basin. The thick light-grey dots in the θ plots represent the stations and bottle sampling spots. The data here plotted is the same used to compute C_{ant} storages and other results presented in this work.

Rhein et al., 2007; Y'08). The described thermohaline evolution concurs with the θ/S results shown by Y'08 for the LSW core: A salinity and temperature minimum is recorded in 1996 at the Irminger Sea (which is two years behind the θ/S minimum at the Labrador Sea). It is followed by a progressive salinization and warming due to lateral mixing that can be observed along the $\sigma_1=36.93$ isopycnal and extends to the rest of LSW density range (Sarfanov et al., 2007; Y'08).

In 1981, there is a manifest stratification between the nearly oxygen-saturated sub-surface waters and the older NEADW that is clearly identified from the AOU profiles. The relative AOU minimum at the bottom of the western part in the Irminger Basin indicates the marked presence of DSO. The C_{ant} concentrations follow a similar pattern to AOU: high values, close to saturation ($32 \mu\text{mol kg}^{-1}$), near the surface and lower values ($\sim 45\%$ of saturation) towards the bottom. During the first deep convection events in the Irminger Sea in the early 1990's there was a significant and parallel increase in the C_{ant} and oxygen loads in the upper 1500 m. Nevertheless, the NEADW region shows higher AOU along with slightly lower (around 15%) C_{ant} values than in 1981, denoting that ventilation does not reach as deep

down. The high ventilation of the water column caused by the strong deep convection between 1991 and 1997 (Lazier et al., 2002) resulted in smaller AOU and higher C_{ant} values during FOUREX than previously recorded for the LSW in the Irminger Basin. In 1997, the C_{ant} concentrations ($30 \pm 0.7 \mu\text{mol kg}^{-1} \approx 80\%$ saturated) at the LSW core is at a maximum and AOU at a minimum. The NEADW layer is richer in oxygen, less saline and it contains about 50% more C_{ant} than in 1991, suggesting that more intense mixing processes occurred with the upper bounding LSW layer. In the Charlie-Gibbs Fracture Zone (CGFZ) the LSW and NEADW normally flow in opposite direction according to general circulation schemes (Schott et al., 2004; Y'08), and mixing processes are enhanced. During 1997 the LSW transport in this area was particularly intense (Lherminier et al., 2007). During the OVIDE period, convection was weak in the Labrador Sea (K'06; Rhein et al., 2007) and no deep convection was recorded in the Irminger Sea (Y'08) resulting in a re-stratification of the water column and an aging of the deep-water masses. This is particularly evident in the cLSW, whose AOU increased by $10 \mu\text{mol kg}^{-1}$ on average from 1997 to 2006. Also, sub-surface (Fig. 1b) C_{ant} levels keep

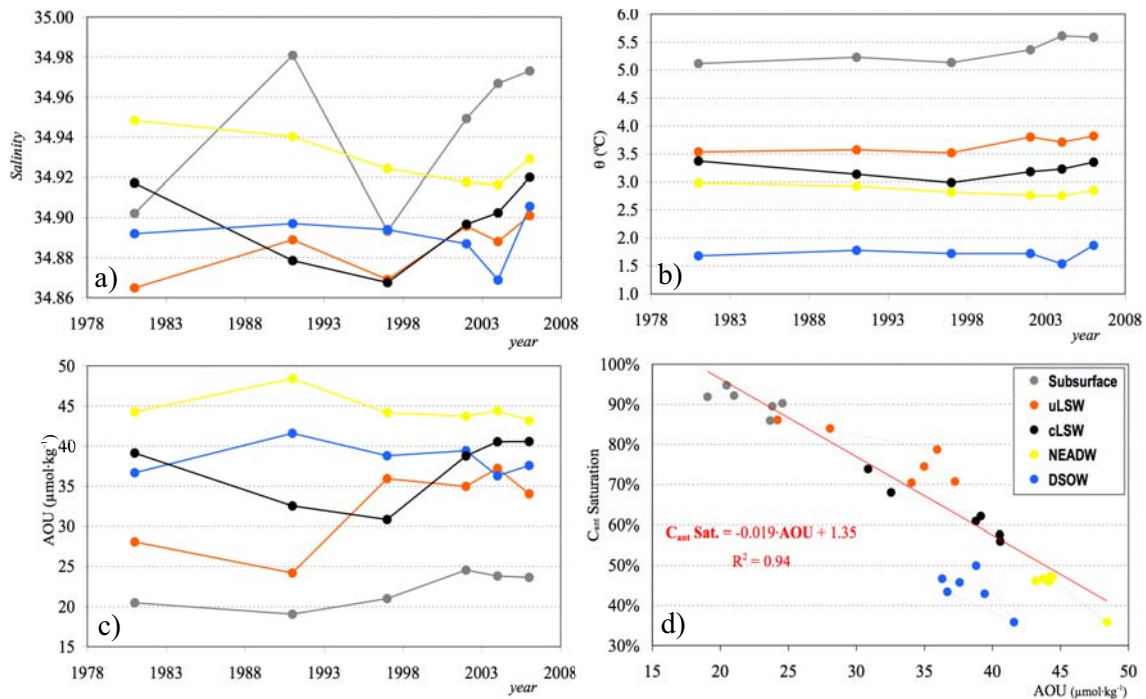


Fig. 3. Data from Table 2 plotted to show the temporal evolution (1981–2006) of the average (a) Salinity, (b) θ (°C) and (c) AOU ($\mu\text{mol}\cdot\text{kg}^{-1}$) of the main water masses in the Irmingier basin. (d) shows the correlation found between AOU and the % saturation concentration of C_{ant} .

rising in response to the atmospheric CO₂ increase. Conversely, weaker winds and buoyancy forcing associated with the low NAO index period during OVIDE provoked an increase in the stratification of the upper layers. This precluded local ventilation and translated into a dilution of C_{ant} in the cLSW layer due to the permanently active isopycnal mixing. The C_{ant} in the NEADW increases continuously suggesting incorporation of young water by entrainment downhill of the Iceland-Scotland sills. Finally, the DSOW flow (Olsson et al., 2005; Tanhua et al., 2008) appears more ventilated with respect to previous years and it also displays small C_{ant} relative maxima. The observed increase of C_{ant} in the NEADW and DSOW can derive from vigorous mixing processes, but it might also reflect the increase of the C_{ant} content in the Arctic source waters.

The average values (from bottle data) and associated uncertainties in salinity, temperature, AOU, C_{ant} and saturation concentration of C_{ant} ($C_{\text{ant}}^{\text{sat}}$) for each cruise and layer (Fig. 1) are summarised on Table 2 and Fig. 3. The average thickness of the layers and their percentage contribution to C_{ant} specific inventories are also given in Table 2. The thickness was calculated as the average distance between layers weighed by the separation between stations. The averages for the rest of properties were computed integrating vertically and horizontally, and then dividing by the area of the corresponding layer. The $C_{\text{ant}}^{\text{sat}}$ is estimated from the average temperature and salinity of the layer, assuming full equilibrium of

surface waters with the average atmospheric molar fraction of CO₂ ($x\text{CO}_2$) at the year of each cruise. A quantitative evaluation of the previously described interdependences between the variability of AOU, C_{ant} and ventilation has been attempted by plotting the percentage of $C_{\text{ant}}^{\text{sat}}$ vs. AOU from Table 2 (Fig. 3d). The term % $C_{\text{ant}}^{\text{sat}}$ is independent of the atmospheric CO₂ increase since it is referred to the $C_{\text{ant}}^{\text{sat}}$ concentration in the corresponding sampling year. In this sense, % $C_{\text{ant}}^{\text{sat}}$ is comparable to oxygen, whose atmospheric concentration is stationary. Hence, it is expected that recently equilibrated (young) waters will have low AOU and high % $C_{\text{ant}}^{\text{sat}}$ values, while the opposite is expected in older waters that have undergone large remineralization of organic matter. We found that the largest temporal variability of AOU and % $C_{\text{ant}}^{\text{sat}}$ is in the cLSW layer, where both variables are highly correlated ($R^2=0.94$). The uLSW shows also a significant % $C_{\text{ant}}^{\text{sat}}$ vs. AOU correlation ($R^2=0.74$). When all Irmingier Sea water masses in Table 2 (except for the DSOW, which represents only 5% of the water column volume) are considered altogether a correlation of $R^2=0.91$ is obtained (Fig. 3d). This suggests that in the Irmingier Sea, % $C_{\text{ant}}^{\text{sat}}$ for the sampling year could be estimated fairly accurately from AOU in the main water masses. Hence, for a given AOU value the % $C_{\text{ant}}^{\text{sat}}$ would be invariable, independently from the sampling year. This AOU vs % $C_{\text{ant}}^{\text{sat}}$ dependence establishes an empirical quantitative relationship based on a simplified mixing model with sub-surface waters and NEADW as end-members. The

former would represent the highly ventilated young waters from the winter mixed layer (WML) whereas the latter would stand for the older components. The deviations from this hypothetical mixing line can be due to lateral advection, to interannual or decadal variability of water mass formation or to differential biological activity rates.

The temporal evolution of the average C_{ant} in each of the five layers is plotted in Fig. 4. The C_{ant} estimation approach used is the φC_T^{O} method (Appendix A). The sub-surface layer (Fig. 1b) increases its C_{ant} steadily and sustains its high % $C_{\text{ant}}^{\text{sat}}$ (>86%) while trying to catch up with the rising atmospheric CO₂ concentrations. The uLSW trend from 1981 to 1991 follows its upper bound sub-surface layer, keeping up with the atmospheric CO₂ increase and maintaining its % $C_{\text{ant}}^{\text{sat}}$. The maximum thinning of the uLSW layer from 1981 to 1997 (Table 2) coincides with the end of the maximum convection period in the Irminger Sea (K'06). The cLSW almost doubled its thickness and average C_{ant} content during this period of time (Table 2 and Fig. 3d) at a rate even superior to the atmospheric one. All of it derives from the increased convection processes that occurred in the NASPG between 1991 and 1997 (K'06). The noteworthy decrease in C_{ant} and layer thickness during the OVIDE cruises caused by the hindered ventilation entails the increase in the AOU levels due to isopycnal mixing. In the NEADW layer, C_{ant} shows a large increment from 1991 to 1997 parallel to the salinity and AOU drop. This suggests the possibility of important diapycnal mixing with the upper re-ventilated cLSW. The DSOW layer will represent a very small contribution (2–3%, Table 2) to C_{ant} storage in the Irminger basin given its small thickness. It shows an analogous behaviour to NEADW, i.e., there is an increase in average C_{ant} from 1991 to 1997, matched with a drop in AOU caused by the incorporation of young water by entrainment downhill of the Iceland-Scotland sills.

Regarding the temporal evolution of the C_{ant} storage rate, a global increase at different paces is observed. From 1981 to 2006 the average rate of increase in the specific C_{ant} inventory for the Irminger Sea has been $1.1 \pm 0.1 \text{ mol C m}^{-2} \text{ yr}^{-1}$. During the early 1990's, this rate was more than twice the mean ($2.3 \pm 0.6 \text{ mol C m}^{-2} \text{ yr}^{-1}$). Compared with this period of exacerbated C_{ant} storage rate in the Irminger Sea, the average storage rate during the following decade (1997–2006) underwent an important fall (Fig. 4) that was estimated in $-1.6 \pm 0.4 \text{ mol C m}^{-2} \text{ yr}^{-1}$. The average C_{ant} storage rate of $0.75 \pm 0.16 \text{ mol C m}^{-2} \text{ yr}^{-1}$ during the FOUREX-OVIDE period was found to be significantly different from that of the early 1990's (p -value < 0.05). Based on the rapid water mass renewal in the Irminger compared to the C_{ant} rate of increase in the ocean, it can be reasonably assumed that the C_{ant} concentrations in the different layers found in the studied section can be extrapolated to the whole Irminger basin. Therefore, the above data was extrapolated to cover the Irminger basin ($0.58 \times 10^6 \text{ km}^2$, taking the FOUREX section and the Denmark Strait as the southern and northern boundaries, respec-

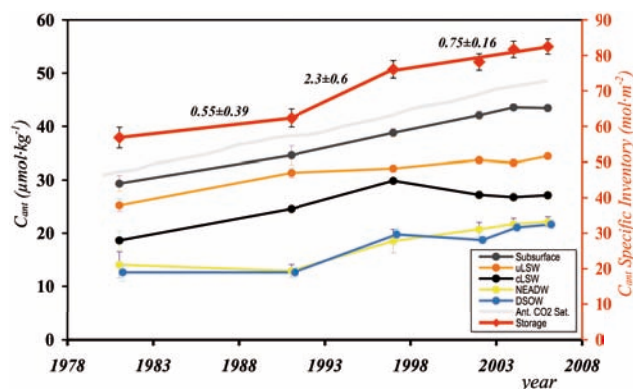


Fig. 4. Temporal evolution (1981–2006) of the average C_{ant} ($\mu\text{mol kg}^{-1}$) stored in the subsurface layer (dark grey line), uLSW (orange line), cLSW (black line), NEADW (yellow line) and DSOW (blue line). The continuous grey line shows the 100% C_{ant} saturation of water masses in equilibrium with the atmosphere over time, following the atmospheric CO₂ increase. The evolution of the specific inventory (in mol C m^{-2}) of C_{ant} in the Irminger basin is given by the thick red line, and its values can be read on the right-hand y-axis. The numbers above this line stand for the rates of increase of C_{ant} storage (in $\text{mol C m}^{-2} \text{ yr}^{-1}$) for the time periods (from left to right) of 1981–1991, 1991–1997 and 1997–2006, respectively.

tively) and give estimates of total inventories, admittedly of the uncertainties attached to this practice. They have been estimated in 0.26 ± 0.02 and $0.38 \pm 0.01 \text{ Gt C}$ for the years 1981 and 2006, respectively.

4 Discussion

As Doney and Jenkins (1988) pointed out, ocean regions affected by strong convection processes tend to acquire large air-sea disequilibria. This applies not only to CO₂, but also to atmospheric gases with higher air-sea transfer velocities such as oxygen or CFCs. The same processes affecting oceanic C_{ant} uptake will be determining the distribution and uptake rates of CFCs. Several works have focused on the CFCs in the NASPG after the 1970's (AS'03; K'07; Rhein et al., 2007), and the patterns they described support the C_{ant} trends obtained in the present study. The above cited works describe how the specific inventories of CFC12 in the core of the cLSW in both the Labrador and Irminger Seas grew until approximately the first half of the 1990's. As Lazier et al. (2002) have illustrated, the formation of cLSW ceased after 1997. The supply shortage of low-salinity/CFC-rich surface waters led to an annual increase in cLSW salinities and a decrease in CFCs because of isopycnal mixing. The CFC12 inventories started to decline strongly from 1997 to 1999 and kept decreasing at a slower rate until 2003 (AS'03; K'07). These evidences seem to correspond with the same pattern here observed for the average C_{ant} in the cLSW,

which decreases from 1997 to 2002 (Fig. 4). According to AS'03, the marked increase in CFC12 concentrations prior to 1995 in the uLSW core reduced to almost standstill from that point until 2000. This result is also in good agreement with the patterns of average C_{ant} obtained for the same years and region in this study (Fig. 4). K'07 have pointed that this significant increase in CFC12 inventories in the uLSW for the NASPG best describes the situation in the Labrador Sea, rather than in the Irminger, where the CFC12 inventory has a more subtle increase during that period. In spite of this remark, our C_{ant} results for the uLSW follow the expected trend, within the associated error margins. With respect to the NEADW and DSOW, AS'03 have shown that, from 1991 to 2000, the CFC12 concentration in the Labrador Sea increased up to 80% in both the NEADW and DSOW layers. Whilst this happened at a steady rate in the case of NEADW, the interannual variability was larger for DSOW. Over the same period, the C_{ant} storages here obtained increased by 50% and 40% in the NEADW and DSOW layers, respectively. There are a few differences in the environmental behavior of CFCs and CO₂ that may account for the dissimilarities in magnitude of their inventories. The former is not affected by the Revelle factor, it has a greater solubility in cold waters and its atmospheric rate of increase is different to that of CO₂.

Although the NASPG has a net gain of C_{ant} by horizontal advection (Mikaloff-Fletcher et al., 2006; Álvarez et al., 2003, hereafter A'03), estimating how much it is stored and how much of that comes from direct exchange with the atmosphere entails certain difficulty. An indirect estimate of the air-sea C_{ant} fluxes can be obtained by combining C_{ant} storage results with horizontal transports into carbon budget balances from closed box studies (as in A'03 and Mikaloff-Fletcher et al., 2006). The C_{ant} storage rate for the Irminger Sea was first estimated by A'03 in $1.5 \pm 0.3 \text{ mol C m}^{-2} \text{ yr}^{-1}$. For that calculation they assumed a fixed C_{ant} rate of increase of $0.85 \mu\text{mol kg}^{-1} \text{ yr}^{-1}$ and estimated also the mean penetration depth (MPD, as in Broecker et al., 1979) using data from the WOCE A20 and FOUREX cruises for the 1990–1997 time period. Assuming a transient steady state (TSS, Keeling and Bolin, 1967) for C_{ant} , the MPD is defined as the quotient between the specific inventory of C_{ant} in the water column and the C_{ant} concentration in the mixed layer ($C_{\text{ant}}^{\text{ml}}$). The model results presented in Tanhua et al. (2006) demonstrate that the TSS assumption is indeed valid for C_{ant} in this part of the North Atlantic Ocean. A high MPD normally indicates that large amounts of C_{ant} have penetrated in the water column following strong vertical convection processes (>1000 m depth) generated in the considered region, and vice versa. A'03 calculated an average and constant MPD for the Irminger basin of $1739 \pm 381 \text{ m}$ by approximating $C_{\text{ant}}^{\text{ml}} \approx C_{\text{ant}}^{\text{sat}}$ in the corresponding sampling years. The average C_{ant} storage rate for the 1981–2006 period in the Irminger Sea here obtained is $1.1 \pm 0.1 \text{ mol C m}^{-2} \text{ yr}^{-1}$. The calculated average MPD for the considered years is

$1715 \pm 63 \text{ m}$. This is quite in agreement with A'03, although the MPD values are seen to vary, especially in the strong convection periods such as from 1991–1997. Also, Tanhua et al. (2006) using an OGCM have shown that deviations from the TSS behaviour are possible in the SPNA due to the variability in deep water formation. Specifically, the MPD in the Irminger basin for the years 1981, 1991, 1997, 2002, 2004 and 2006 are, respectively: 1835 ± 140 , 1657 ± 88 , 1808 ± 72 , 1678 ± 56 , 1679 ± 54 and $1632 \pm 42 \text{ m}$. The $1.5 \pm 0.3 \text{ mol C m}^{-2} \text{ yr}^{-1}$ estimate from A'03 is larger than the average $1.1 \pm 0.1 \text{ mol C m}^{-2} \text{ yr}^{-1}$ here obtained and, anyhow, lower than the estimated rate, between 1991 and 1997, of $2.3 \pm 0.6 \text{ mol C m}^{-2} \text{ yr}^{-1}$. Some factors accounting for the temporal variability of C_{ant} storage rates may explain some of these discrepancies, primarily: a) The time variability of the MPD can affect notoriously the C_{ant} storage rates, especially between 1991 and 1997 (8% larger than the average). There can exist exceptional interannual stages where the storage rates can amount up to twice (1991–1997) or almost half (1997–2006) the long-term average; b) The C_{ant} rate of increase must consider the dependence of the $C_{\text{ant}}^{\text{sat}}$ with temperature, which is intimately connected with the Revelle factor (it describes how the $p\text{CO}_2$ in seawater changes for a given change in C_T , and vice versa). The capacity for ocean waters to take up C_{ant} is inversely proportional to the Revelle factor, which depends on temperature. The C_{ant} rates of storage can change $\sim 2\%$ per °C.

Our observations in the Irminger Sea can also be compared with other works on the secular variation of sea surface $p\text{CO}_2$ that cover larger areas. In the NASPG, Lefèvre et al. (2004) reported a mean increase of $1.8 \mu\text{atm yr}^{-1}$ between 1982 and 1998. This corresponds to a $\Delta C_T = 0.77 \mu\text{mol kg}^{-1}$ per annum for an average sea surface temperature of 5°C in the Irminger Sea. If an average MPD of 1715 m is considered for this region and time period, the above $\Delta p\text{CO}_2$ translates into a C_{ant} storage rate that increases by $1.35 \text{ mol C m}^{-2} \text{ yr}^{-1}$. This is very close to the $1.22 \pm 0.03 \text{ mol C m}^{-2} \text{ yr}^{-1}$ estimated here from Fig. 4 for the 1981–1997 period. From sea surface $p\text{CO}_2$ measurements Schuster and Watson (2007) showed that the sink of atmospheric CO₂ in the whole North Atlantic was subject to important interannual variability. They estimated an annual decrease of the North Atlantic uptake of $-1.1 \text{ mol C m}^{-2} \text{ yr}^{-1}$ between 1997 and the mid-2000's. They argued that the main causes for this change were the declining rates of wintertime mixing and ventilation between surface and subsurface waters due to increasing stratification. In the present work we have estimated this same rate of decrease to be $-1.6 \pm 0.4 \text{ mol C m}^{-2} \text{ yr}^{-1}$ for the 1997–2006 decade in the Irminger Sea. Corbière et al. (2007) estimated an annual increase in wintertime sea surface $p\text{CO}_2$ of $3.0 \mu\text{atm yr}^{-1}$ between 1993 and 2003 utilizing data from a shipping route from Iceland to Newfoundland. They attributed this finding principally to the increasing sea surface temperatures linked with the shift of the NAO index into a negative phase after

wintertime 1995. According to Schuster and Watson (2007), this corresponds to an annual decrease of the C_{ant} storage of $-1.6 \text{ mol C m}^{-2} \text{ yr}^{-1}$, which is in excellent agreement with our estimates.

In summary, the general decline of the NASPG CO₂ sink is supported by the data here obtained and it is corroborated by other results like those from Schuster and Watson (2007) or Corbière et al. (2007). There is a documented variability of the Labrador Sea deep convection that reached its maximum activity during the early to mid 1990s, correlated with positive NAO phases. The maximum C_{ant} storage rate occurred during this maximum convection period. The observed convection decrease since 1997 in the NASPG is mainly tied to the enhanced stratification and the consequent reduced heat loss in the northern North Atlantic (Lazier et al., 2002; AS'03; K'07). All these fluctuations are embodied in the NAO index variability. The above factors have a direct influence on the physical pump of CO₂ and add to the changes in the buffer capacity of surface waters to aggravate the capacity of the North Atlantic as a CO₂ sink.

Appendix A

The φC_T° method (Vázquez-Rodríguez et al., 2008a) is a process-oriented biogeochemical approach to estimate C_{ant} . It is an alternative to existing process-based C_{ant} estimation methods such as the ΔC^* (GSS'96) or TrOCA (Touratier et al., 2007). The distinctive characteristics of the φC_T° method are:

1. The sub-surface layer (100–200 m) is taken as a reference for characterising the properties of the water masses at their respective formation times. The variability of the conservative properties of greatest importance in C_{ant} estimation (θ , S , NO, PO) is at least one order of magnitude smaller than in the surface layer. In addition, the thermohaline variability of the surface layer encloses and represents all water masses outcropped in the Atlantic Ocean. The use of data from the sub-surface layer reduces the sparseness of data available for parameterizations given the high amount of data for sub-surface waters at any season compared to the scarce surface winter data.
2. The air-sea disequilibrium (ΔC_{dis}) is parameterized at the sub-surface layer first using a short-cut method to estimate C_{ant} . Since the average age of the water masses in the 100–200 m depth domain, and most importantly in outcropping regions, is under 25 years, the use of the short-cut method to estimate C_{ant} is appropriate (Matear et al., 2003).
3. The A_T° and ΔC_{dis} parameterizations (in terms of conservative tracers) obtained from sub-surface data are applied directly to calculate C_{ant} in the water column for

waters above the 5°C isotherm and via an OMP approach (like in GSS'96) for waters with $\theta < 5^{\circ}\text{C}$. This approach especially improves the estimates in cold deep waters that are subject to strong and complex mixing processes and represent an enormous volume of the global ocean (~86%). One important aspect in this process is that, unlike for the ΔC^* method, CFC data are not necessary to make C_{ant} predictions, since none of the A_T° or ΔC_{dis} parameterizations are CFC-reliant.

Following the work from Matsumoto and Gruber (2005), the φC_T° method proposes an approximation to the horizontal (spatial) and vertical (temporal) variability of ΔC_{dis} ($\Delta \Delta C_{\text{dis}}$) in the Atlantic Ocean in terms of C_{ant} and ΔC_{dis} itself. Also, the decrease of preindustrial A_T° due to CaCO₃ dissolution changes projected from models (Heinze, 2004) and the effect of rising sea surface temperatures on the parameterized A_T° were corrected in our calculations. These two last corrections are minor and would be very difficult to quantify directly through measurements. However, they should still be considered if a maximum $4 \mu\text{mol kg}^{-1}$ bias ($2 \mu\text{mol kg}^{-1}$ on average) in C_{ant} estimates wants to be avoided. Following several in-detail evaluations of the uncertainties in C_{ant} evaluation through back-calculation approaches (Gruber et al., 1996; Gruber, 1998; Sabine et al., 1999; Wanninkhof et al., 2003; Lee et al., 2003), random errors were propagated over the precision limits of the various measurements required for solving their C_{ant} estimation equations. The A_T° parameterization here obtained has an associated uncertainty two times lower than in GSS'96, while the uncertainties for ΔC_{dis} vary between 4 and $7 \mu\text{mol kg}^{-1}$ (average $5.6 \mu\text{mol kg}^{-1}$). The overall uncertainty in C_{ant} determination of the φC_T° method is $5.2 \mu\text{mol kg}^{-1}$.

A recent inter-comparison study of several C_{ant} back-calculation methods (Vázquez-Rodríguez et al., 2008b) has shown how North Atlantic C_{ant} inventory estimates from the φC_T° method are in close agreement with results from the TTD method (Vaughan et al., 2006) and in reasonable agreement with ΔC^* estimates as of Lee et al. (2003). The TrOCA approach (Touratier et al., 2007) produced C_{ant} inventories that are higher on average than the three methods previously mentioned. There exist discrepancies amongst all of the above-cited methods, but the main results obtained in the present study are independent of the choice of C_{ant} reconstruction method. For comparison, the rates of change of the C_{ant} storage calculated with the φC_T° method in the present work were also calculated using the TrOCA method. The general trends of temporal evolution (1981–2006) in C_{ant} storage rates as from either method appear to be in very good agreement: 1.07 ± 0.14 and $1.14 \pm 0.23 \text{ mol C m}^{-2} \text{ yr}^{-1}$ for the φC_T° and TrOCA method, respectively (correlation coefficient $R^2=0.97$; $N=6$). During the high NAO phase from 1991 to 1997, the C_{ant} storage rates of change predicted to be more than twice the average, irrespective of the C_{ant} method chosen (2.3 ± 0.6 and $3.3 \pm 0.6 \text{ mol C m}^{-2} \text{ yr}^{-1}$

for φC_T° and TrOCA, respectively). In the low NAO phase (1997–2006), the rates of change are seen to decrease in both cases: $0.75 \pm 0.16 \text{ mol C m}^{-2} \text{ yr}^{-1}$ according to φC_T° and $0.5 \pm 0.4 \text{ mol C m}^{-2} \text{ yr}^{-1}$ according to the TrOCA approach.

Acknowledgements. This work was developed and funded by the OVIDE research project from the French research institutions IFREMER and CNRS/INSU and by the European Commission within the 6th Framework Programme (EU FP6 CARBOOCEAN Integrated Project, Contract no. 511176). We would like to extend our gratitude to two anonymous reviewers for their constructive and careful comments. Marcos Vázquez-Rodríguez is funded by Consejo Superior de Investigaciones Científicas (CSIC) I3P predoctoral grant program REF.: I3P-BPD2005.

Edited by: F. Joos

References

- Álvarez, M., Ríos, A. F., Pérez, F. F., Bryden, H. L., and Rosón, G.: Transports and budgets of total inorganic carbon in the subsolar and temperate North Atlantic, *Global Biogeochem. Cy.*, 17(1), 1002, doi:10.1029/2002GB001881, 2003.
- Azetsu-Scott, K., Jones, E. P., Yashayaev, I., and Gershey, R. M.: Time series study of CFC concentrations in the Labrador Sea during deep and shallow convection regimes (1991–2000), *J. Geophys. Res.*, 108(C11), 3354, doi:10.1029/2002JC001317, 2003.
- Böning C. W., Scheinert, M., Dengg, J., Biastoch, A., and Funk, A.: Decadal variability of subpolar gyre transport and its reverberation in the North Atlantic overturning, *Geophys. Res. Lett.*, 33, L21S01, doi:10.1029/2006GL026906, 2006.
- Broecker, W. S., Takahashi, T., Simpson, H. J., and Peng, T. H.: Fate of fossil fuel carbon dioxide and the global carbon budget, *Science*, 206, 409–418, 1979.
- Bryden, H. L., Longworth, H. R., and Cunningham, S. A.: Slowing of the Atlantic meridional overturning circulation at 25°N, *Nature*, 438, 655–657, 2005.
- Canadell, J., Le Quééré, C., Raupach, M. R., Fields, C., Buitenhuis, E. T., Ciais, P., Conway, T. J., Gillett, N. P., Houghton, R. A., and Marland, G.: Contributions to accelerating atmospheric CO₂ growth from economic activity, carbon intensity, and efficiency of natural sinks, *P. Natl. Acad. Sci. USA*, 104(47), 18866–18870, doi:10.1073/pnas.0702737104, 2007.
- Corbière, A., Metzl, N., Reverdin, G., Brunet, C., and Takahashi, T.: Interannual and decadal variability of the oceanic carbon sink in the North Atlantic subpolar gyre, *Tellus*, 59, 167–167, DOI: 10.1111/j.1600-0889.2006.00232, 1–11, 2007.
- Cubasch, U., Meehl, G. A., Boer, G. J., Stouffer, R. J., Dix, M., Noda, A., Senior, C. A., Raper, S., Yap, K. S., Abe-Ouchi, A., et al.: *Climate Change 2001: The Scientific Basis*, edited by: Houghton, J. T., Ding, Y., Griggs, D. J., Noguer, M., van der Linden, P. J., Dai, X., Maskell, K., and Johnson, C. A., Cambridge Univ. Press, Cambridge, UK, 525–582, 2001.
- Curry, R., McCartney, M. S., and Joyce, T. M.: Oceanic transport of subpolar climate signals to mid-depth tropical waters, *Nature*, 391, 575–577, 1998.
- Dickson, R. R., Lazier, J. R. N., Meincke, J., Rhines, P. B., and Swift, J. H.: Long-term coordinated changes in the convective activity of the North Atlantic, *Prog. Oceanogr.*, 38, 241–295, 1996.
- Doney, S. C. and Jenkins, W. J.: The effect of boundary conditions on tracer estimates of thermocline ventilation rates, *J. Mar. Res.*, 46, 947–965, 1988.
- Drijfhout, S. S. and Hazeleger, W.: Changes in MOC and gyre-induced Atlantic Ocean heat transport, *Geophys. Res. Lett.*, 33, L07707, doi:10.1029/2006GL025807, 2006.
- Duce, R. A., LaRoche, J., Altieri, K., Arrigo, K. R., et al.: Impacts of atmospheric anthropogenic nitrogen in the open ocean, *Science*, 320, 893–897, 2008.
- Falina, A., Sokov, A., and Sarafanov, A.: Variability and renewal of Labrador Sea Water in the Irminger Basin in 1991–2004, *J. Geophys. Res.*, 112, C01006, doi:10.1029/2005JC003348, 2007.
- Gruber, N., Sarmiento, J. L., and Stocker, T. F.: An improved method for detecting anthropogenic CO₂ in the oceans, *Global Biogeochem. Cy.*, 10, 809–837, 1996.
- Gruber, N.: Anthropogenic CO₂ in the Atlantic Ocean, *Global Biogeochem. Cy.*, 12, 165–191, 1996.
- Häkkinen, S. and Rhines, P. B.: Decline of the subpolar North Atlantic circulation during the 1990s, *Science*, 204, 555–559, 2004.
- Hátún, H., Sandø, A. B., Drange, H., Hansen, B., and Valdimarsson, H.: Influence of the Atlantic Subpolar Gyre on the thermohaline circulation, *Science*, 309, 1841–1844, 2005.
- Heinze, C.: Simulating oceanic CaCO₃ export production in the greenhouse, *Geophys. Res. Lett.*, 31, L16308, doi:10.1029/2004GL020613, 2004.
- Joos, F., Plattner, G.-K., Stocker, T. F., Marchal, O., and Schmittner, A.: Global warming and marine carbon cycle feedbacks on future atmospheric CO₂, *Science*, 284, 464–467, 1999.
- IPCC (2007): *Climate Change: The Physical Science Basis*, Contribution of Working Group I to the Fourth Assessment Report of Intergovernmental Panel on Climate Change, 940 pp., Cambridge University Press, Cambridge, UK, 2007.
- Keeling, C. D. and Bolin, B.: The simultaneous use of chemical tracers in oceanic studies, *Tellus*, 19, 566–581, 1967.
- Kieke, D., Rhein, M., Stramma, L., Smethie, W. M., LeBel, D. A., and Zenk, W.: Changes in the CFC inventories and formation rates of Upper Labrador Sea Water, 1997–2001, *J. Phys. Oceanogr.*, 36, 64–86, 2006.
- Kieke, D., Rhein, M., Stramma, L., Smethie, W. M., Bullister, J. L., and LeBel, D. A.: Changes in the pool of Labrador Sea Water in the subpolar North Atlantic, *Geophys. Res. Lett.*, 34, L06605, doi:10.1029/2006GL028959, 2007.
- Latif, M., Böning, C. W., Willebrand, J., Biastoch, A., Dengg, J., Keenlyside, N., and Schweckendiek, U.: Is the thermohaline circulation changing?, *J. Climate*, 19, 4631–4637, 2006.
- Lazier, J., Hendry, R., Clarke, R. A., Yashayaev, I., and Rhines, P.: Convection and restratification in the Labrador Sea, 1990–2000, *Deep-Sea Res.*, 49, 1819–1835, 2002.
- Lee, K., Choi, S.-D., Park, G.-H., Wanninkhof, R., Peng, T.-H., Key, R. M., Sabine, C. L., Feely, R. A., Bullister, J. L., Millero, F. J., and Kozyr, A.: An updated anthropogenic CO₂ inventory in the Atlantic Ocean, *Global Biogeochem. Cy.*, 17(4), 1116, doi:10.1029/2003GB002067, 2003.
- Lefèvre, N., Watson, A. J., Olsen, A., Ríos, A. F., Pérez, F. F., and Johannessen, T.: A decrease in the sink for atmospheric CO₂ in the North Atlantic, *Geophys. Res. Lett.*, 31, L07306, 1–4, doi:10.1029/2003GL018957, 2004.

- Lherminier, P., Mercier, H., Gourcuff, C., Alvarez, M., Bacon, S., and Kermabon, C.: Transports across the 2002 Greenland-Portugal Ovide section and comparison with 1997, *J. Geophys. Res.*, 112, C07003, doi:10.1029/2006JC003716, 2007.
- Matear, R. J., Wong, C. S., and Xie, L.: Can CFCs be used to determine anthropogenic CO₂?, *Global Biogeochem. Cy.*, 17(1), 1013, doi:10.1029/2001GB001415, 2003.
- Matsumoto, K. and Gruber, N.: How accurate is the estimation of anthropogenic carbon in the ocean? An evaluation of the ΔC^* method, *Global Biogeochem. Cy.*, 19, GB3014, doi:10.1029/2004GB002397, 2005.
- Mikaloff-Fletcher, S. E., Gruber, N., Jacobson, A. R., Doney, S. C., Dutkiewicz, S., Gerber, M., Follows, M., Joos, F., Lindsay, K., Menemenlis, D., Mouchet, A., Müller, S. A., and Sarmiento, J. L.: Inverse estimates of anthropogenic CO₂ uptake, transport, and storage by the ocean, *Global Biogeochem. Cy.*, 20, GB2002, doi:10.1029/2005GB002530, 2006.
- Olsson, K. A., Jeansson, E., Tanhua, T., and Gascard, J. C.: The East Greenland Current studied from CFCs, *J. Marine Syst.*, 55, 77–95, 2005.
- Pickart, R. S., Spall, M. A., and Lazier, J. R. N.: Mid-depth ventilation in the western boundary current system of the sub-polar gyre, *Deep-Sea Res. I*, 44, 1025–1054, 1997.
- Pickart, R. S., Straneo, F., and Moore, G. W. K.: Is Labrador Sea Water formed in the Irminger Basin?, *Deep Sea Res. I*, 50, 23–52, 2003.
- Rhein, M., Kieke, D., and Steinfeldt, R.: Ventilation of the Upper Labrador Sea Water, 2003–2005, *Geophys. Res. Lett.*, 34, L06603, doi:10.1029/2006GL028540, 2007.
- Sabine, C. L., Key, R. M., Johnson, K. M., Millero, F. J., Poisson, A., Sarmiento, J. L., Wallace, D. W. R., and Winn, C. D.: Anthropogenic CO₂ inventory of the Indian Ocean, *Global Biogeochem. Cy.*, 13, 179–198, 1999.
- Sabine, C. L., Feely, R. A., Gruber, N., Key, R. M., Lee, K., Bullister, J. L., Wanninkhof, R., Wong, C. S., Wallace, D. W. R., Tilbrook, B., Millero, F. J., Peng, T.-H., Kozyr, A., Ono, T., and Ríos, A. F.: The oceanic sink for anthropogenic CO₂, *Science*, 305, 367–371, 2004.
- Sarafanov, A., Sokov, A., Demidov, A., and Falina, A.: Warming and salinification of intermediate and deep waters in the Irminger Sea and Iceland Basin in 1997–2006, *Geophys. Res. Lett.*, 34, L23609, doi:10.1029/2007GL031074, 2007.
- Sarmiento, J. L. and Le Quéré, C.: Oceanic carbon dioxide uptake in a model of century-scale global warming, *Science*, 274, 1346–1350, 1996.
- Schott, F. A., Zantopp, R., Stramma, L., Dengler, M., Fischer, J., and Wibaux, M.: Circulation and Deep-Water Export at the Western Exit of the Subpolar North Atlantic, *J. Phys. Oceanogr.*, 34, 817–843, 2004.
- Schuster, U. and Watson, A. J.: A variable and decreasing sink for atmospheric CO₂ in the North Atlantic, *J. Geophys. Res.*, 112, C11006, doi:10.1029/2006JC003941, 2007.
- Stramma, L., Kieke, D., Rhein, M., Schott, F., et al.: Deep Water changes at the western boundary of the subpolar North Atlantic, 1996–2001, *Deep Sea Res. I*, 51, 1033–1056, 2004.
- Tanhua, T. and Wallace, D. W. R.: Consistency of TTO-NAS inorganic carbon data with modern measurements, *Geophys. Res. Lett.*, 32, L14618, doi:10.1029/2005GL023248, 2005.
- Tanhua, T., Biastoch, A., Körtzinger, A., Lüger, H., Böning, C., and Wallace, D. W. R.: Changes of anthropogenic CO₂ and CFCs in the North Atlantic between 1981 and 2004, *Global Biogeochem. Cy.*, 20, GB4017, doi:10.1029/2006GB002695, 2006.
- Tanhua, T., Olsson, K. A., and Jeansson, E.: Tracer evidence of the origin and variability of Denmark Strait Overflow Water, in: *Arctic-Subarctic Ocean Fluxes: Defining the role of the Nordic Seas in Climate*, edited by: Dickson, R. R., Meincke, J., and Rhines, P., 475–503, Springer Verlag, 2008.
- Touratier, F., Azouzi, L., and Goyet, C.: CFC-11, $\Delta^{14}C$ and 3H tracers as a means to assess anthropogenic CO₂ concentrations in the ocean, *Tellus*, 59B, 318–325, DOI: 10.1111/j.1600-0889.2006.00247.x, 2007.
- Vázquez-Rodríguez, M., Padin, X. A., Pérez, F. F., Ríos, A. F., and Bellerby, R. G. J.: Anthropogenic carbon determination from sub-surface boundary conditions, *J. Marine Syst.*, submitted, 2008a, available at: <http://store.pangaea.de/Projects/CARBOOCEAN/MastersThesisRodriguez.pdf>.
- Vázquez-Rodríguez, M., Touratier, F., Lo Monaco, C., Waugh, D. W., Padin, X. A., Bellerby, R. G. J., Goyet, C., Metzl, N., Ríos, A. F., and Pérez, F. F.: Anthropogenic carbon distributions in the Atlantic Ocean: Databased estimates from the Arctic to the Antarctic, *Biogeosciences Discuss.*, 5, 1421–1443, 2008b, <http://www.biogeosciences-discuss.net/5/1421/2008/>.
- Wallace, D. W. R.: Storage and transport of excess CO₂ in the oceans: the JGOFS/WOCE Global CO₂ Survey, in: *Ocean Circulation and Climate*, edited by: Church, J., Siedler, G., and Gould, J., Academic Press, 489–521, US JGOFS Contribution No. 953, 2001.
- Wanninkhof, R., Peng, T. H., Huss, B., Sabine, C. L., and Lee, K.: Comparison of inorganic carbon system parameters measured in the Atlantic Ocean from 1990 to 1998 and recommended adjustments, ORNL/CDIAC-140, 43 pp., Oak Ridge Natl. Lab., US Dept. of Energy, Oak Ridge, Tenn., 2003.
- Watson, A. J., Nightingale, P. D., and Cooper, D. J.: Modeling atmosphere-ocean CO₂ transfer, *Philos. T. Roy Soc. B*, 348, 125–132, 1995.
- Yashayev, I., Penny Holliday, N., Bersch, M., and van Aken, H. M.: The history of the Labrador Sea Water: Production, Spreading, Transformation and Loss, in: *Arctic-Subarctic Ocean Fluxes: defining the role of the Northern Seas in climate*, edited by: Dickson, R. R., Meincke, J., and Rhines, P., Springer, The Netherlands, 569–612, 2008.